Asian Journal of Chemistry; Vol. 25, No. 3 (2013), 1410-1414

ASIAN JOURNAL OF CHEMISTRY

http://dx.doi.org/10.14233/ajchem.2013.13044

First-Principles Study of Ni_2CrAl Intermetallic Compound with Non-Heusler Phase

HAI-LI YU[1], XIAO-HUI DUAN[1,*], YONG-JUN MA[1], XU-HAN CAO[1] and WEN-JUN ZHU[2]

[1]State Key Laboratory Cultivation Base for Nonmetal Composites and Functional Materials, Southwest University of Science and Technology, Mianyang 621010, P.R. China
[2]Institute of Fluid Physics, China Academy of Engineering Physics, Mianyang 621900, P.R. China

*Corresponding author: Fax: +86 186 2419201; Tel: +86 186 2485116; E-mail: duanxiaohui@swust.edu.cn

(*Received*: 9 November 2011; *Accepted*: 8 September 2012) AJC-12127

The physical properties, such as electronic, elastic and optical properties of Ni_2CrAl intermetallic compound with non-Heusler phase have been investigated using first principles based on density functional theory. The calculated elastic constants indicate that Ni_2CrAl is mechanically stable. The polycrystalline elastic modulus and Poisson's ratio have been deduced by Voigt-Reuss-Hill approximations. According to the calculated ratio of bulk modulus to shear modulus, Ni_2CrAl may be of potential application for ductile materials. The analysis for the band structure reveals that this compound is a conductor. The optical properties have been investigated and the results show Ni_2CrAl can strongly reflect the radiation. This is the first theoretical prediction for the properties of Ni_2CrAl intermetallic compound with non-Heusler phase and the results need experimental confirmation.

Key Words: First-principles, Ni_2CrAl intermetallic compound, Mechanical properties, Electric properties, Optical properties.

INTRODUCTION

In recent years, intermetallic compounds have been received more and more attentions. They have been applied as magnetic materials[1], shape memory alloys[2], coating materials[3], hydrogen storage[4] and high temperature structural materials[5]. Among these intermetallic compounds, Ni-Al intermetallic compounds are the promising candidates as structure materials in aerospace industry and for nano-technological applications with recent examples of applications of bimetallic Ni-Al reactive nanostructure as nano-heaters[6]. The attractive properties of these intermetallic compounds include low density, good creep strength and high temperature oxidation resistance. In addition, these intermetallic compounds also show good mechanical properties over a wide temperature range, which are crucial from the technological point of view. Nevertheless, there are also some disadvantages for them. For example, their resistance to oxidation attack is insufficient. Meanwhile, they are brittle at room temperature, which restricts their application in material fields.

In order to overcome these problems, some alloying elements such as Fe, Cr, Co, Cu and Mn were found useful in improving the ductility of Ni-Al alloys. Ni-Al-based ternary Ni-Al-Fe intermetallic compounds show good plasticity and one-way, as well as two-way shape memory effect[7]. Besides, some promising ternary Ni-Al-based intermetallic compounds such as Ni-Al-Cr ternary system were developed to solve the problems. The Ni-Al-Cr ternary intermetallic compounds have been widely investigated experimentally and theoretically. For example, Choe's group synthesized Ni-Cr-Al superalloy foam successfully[8] and the structure and mechanical properties of the superalloy foam were also investigated. Jiang's group investigated the site preference of Cr in B2 NiAl[9]. The results showed that the site occupancy of Cr in B2 NiAl was a strong function of both alloy composition and temperature. However, up to date, the reports on the experimental preparation of Ni-Cr-Al intermetallic compounds are limited to $NiAl_5Cr_5$, $NiAl_5Cr_{10}$, $NiAl_{10}Cr_3$ and $NiAl_3Cr_{12}$[10]. Other Ni-Cr-Al ternary intermetallic compounds such as Ni_2CrAl has not been exploited widely. This might be due to the lack of facile and reliable procedures for preparing other Ni-Cr-Al intermetallic compounds.

The structure of Ni_2CrAl has two types, including Heusler phase and non-Heusler phase. Heusler alloys exhibit very interesting magnetic and electric properties, which are ferromagnetic metal alloys based on Heusler phase. Heusler phases are intermetallics with particular composition and face-centered cubic crystal structure. The majority of Heusler alloys order ferromagnetically and saturate in weak applied magnetic fields[11]. Such materials have been experimentally prepared and theoretically studied[4,12,13]. The properties of Ni_2CrAl with Heusler phase have also been theoretically studied by previous

researchers[14,15]. However, to the best of our knowledge, the Ni_2CrAl with non-Heusler phase is not studied to date. A number of properties of that structure are still unknown. In order to take advantage of the properties of these compounds for eventual technological applications, it is necessary to explore various properties by theoretical predication firstly. For this purpose, we use the first-principle method, which is one of the most powerful tools for carrying out theoretical studies of some physical properties[16,17], to predict various physical properties of Ni_2CrAl intermetallic compound with non-Heusler phase.

EXPERIMENTAL

Our first-principles calculations are performed with the CASTEP (Cambridge serial total energy package) code in Materials Studio 3.0 (MS) software[18]. In this code, the Kohn-Sham equations are solved within the framework of density functional theory[19,20] by expanding the wave functions of valence electrons in a basis set of plane waves with kinetic energy smaller than a specified cut-off energy, E_{cut}. The presence of tightly-bound core electrons is represented by non-local ultra-soft pseudo-potentials of the Vanderbilt-type[21]. The states Al $3s^2 3p^1$, Ni $4s^2 3d^8$ and Cr $4s^1 3d^5$ are treated as valence states. The integrations over the Brillouin zone are replaced by discrete summation over special set of k points using Monkhorst-Pack scheme[22]. A plane wave cut-off energy of 400 eV and a 8 × 8 × 8 grid of Monkhorst-Pack points have employed in this study to ensure well convergence of the computed structures and energies. For the calculation of the optical properties, which usually requires a dense mesh of uniformly distributed k-points, the Brillouin zone integration is performed using a 16 × 16 × 16 grid of Monkhorst-Pack points. The exchange-correlation potential is treated within the generated gradient approximation using the scheme of Perdew-Burke-Ernzerhof[23]. The structural parameters of Ni_2CrAl are determined using the Broyden-Fletcher-Goldfarb-Shenno (BFGS) minimization technique, with the following thresholds for converged structures: energy change per atom less than 1×10^{-5} eV, residual force less than 0.03 eV/Å, the displacement of atoms during the geometry optimization less than 0.001 Å and the total stress tensor is reduced to the order of 0.05 GPa by using the finite basis set corrections.

RESULTS AND DISCUSSION

Structural optimization: The space group of Ni_2CrAl structure is Fm-3 m (space group number is 225). The model of Ni_2CrAl cell with non-Heusler phase is shown in Fig. 1, with the atoms in (0, 0, 0) Al, (0.5, 0.5, 0.5) Cr and (0.25, 0.25, 0.25) Ni positions. The lattice parameters of Ni_2CrAl have been optimized in this work. The optimized result is 0.5752 nm in good agreement with the literature value of 0.5737 nm[24]. This confirms proposed computational methodology is suitable for current purpose and the results from geometry optimizations are reliable.

Electronic properties and band structure: The band structure, the density of states (DOS) and partial density of states (PDOS) curves of Ni_2CrAl compound have been calculated, which provide information on the physical basis for stabilizing effect and site occupancy behaviours of materials.

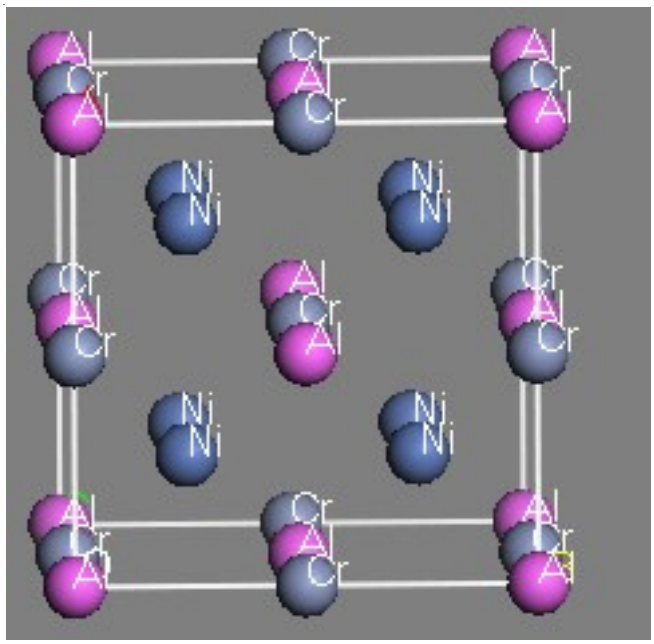

Fig. 1. Model of Ni_2CrAl intermetallic compound cell

The calculated band structure is shown in Fig. 2. The non-existence of a gap at Fermi level (EF, which is located at 0 eV) confirms the metallic character and indicates the intermetallic compound studied here is a conductor.

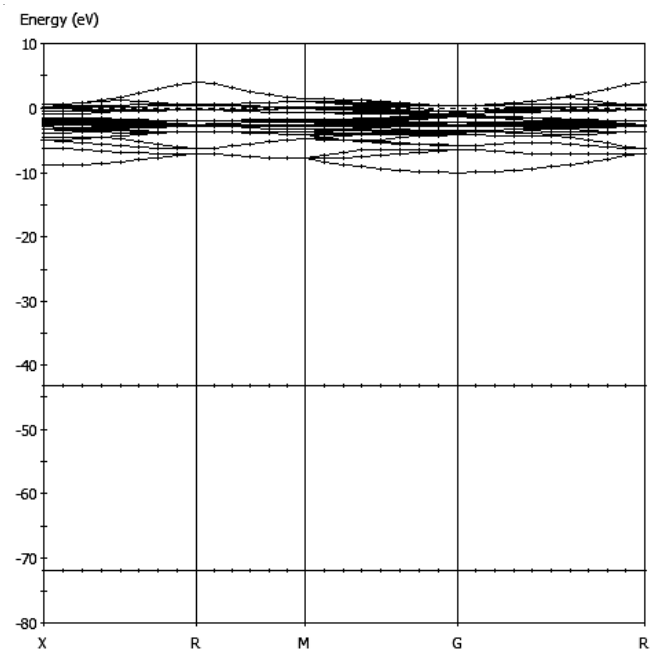

Fig. 2. Calculated band structure of Ni_2CrAl intermetallic compound

To further elucidate the nature of the electronic band structure, the density of states of Ni_2CrAl compound as well as the partial density of states of Ni, Cr and Al in Ni_2CrAl are discussed. The calculated results are presented in Fig. 3. We can identify the angular momentum character of the different structures from the partial density of states. In general, the lower valence band is dominated by *s*-states or *p*-states of the different elements of compounds. From Fig. 3(a) and Fig. 3(d), it can be seen that Al atoms contribute little to valence band

and conduction band. For the partial density of states of Cr, the *s*-states are dominating at energy under -3.5 eV. At the Fermi level, the partial density of states is mainly derived from *d*-states. As far as Ni is concerned, the *p* and *d*-states dominate all the valence band and conduction band. Also, at the Fermi energy, the *d*-states mainly contribute to the partial density of states and contributing from Ni *s* and *p*-states could be neglected.

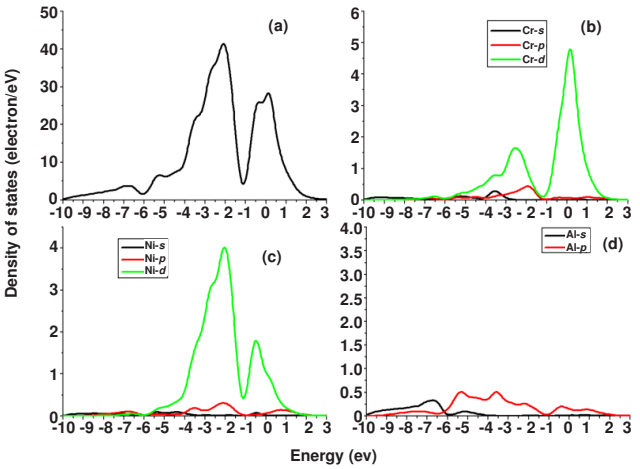

Fig. 3. Calculated total and partial density of states of Ni_2CrAl intermetallic compound

In regard to the density of states curve of Ni_2CrAl, it is seen that there are two bonding peaks below the Fermi level. A strong peak located at -2.1 eV is contributed by the hybridization of Ni *d*-states with Cr *d*-states and a relative weak peak located at -0.35 eV is contributed by the hybridization of Cr *d*-states with Ni *d*-states and little Al *p*-states. Beyond the Fermi level, the density of states is mainly dominated by Cr *d*-states and light Ni *d*-states. The entire conduction region beyond the Fermi level mostly result from Cr *d*-states with small contribution from Ni *d*, Ni *p*-states and Al *p*-states. The density of states value corresponding to the Fermi level [$N(E_F)$] is 27 states/eV. By virtue of analysis of the partial density of states curves, the Cr *d*-states contribute mostly to $N(E_F)$.

Optical properties: From the viewpoint of quantum mechanics, the interaction of a photon with an electron in the system is described in terms of time-dependent perturbations of the ground electronic state. Transitions between occupied and unoccupied states are caused by the photon absorption or emission. The spectra resulting from excitations can be thought of as a joint density of states between the conduction band and the valence band. The imaginary part [$\varepsilon_2(\omega)$] of the dielectric function can be written as:

$$\varepsilon_2(q \to O_{\hat{u}}, h\omega) = \frac{2\pi e^2}{\Omega\varepsilon_0}\sum\left|\left\langle \Psi_K^C \middle| u \cdot r \middle| \Psi_K^V \right\rangle\right|^2 \delta(E_K^C - E_K^V - E) \quad (1)$$

where, u is the vector defining the polarization of the incident electric field; k is the reciprocal lattice vector; the superscripts c and v represent the conduction band and valance band, respectively; and ω is the frequency of the incident photon. Since the dielectric function shows a causal response, the real part $\varepsilon_1(\omega)$ of the dielectric function can be obtained from the imaginary part with the Kramers-Kronig relations. Then the other optical spectra, such as absorption coefficient α(ω), reflectivity R(ω) refractivity index n(ω) and energy-loss L(ω) can be deduced from the values of $\varepsilon_1(\omega)$ and $\varepsilon_2(\omega)$[25]:

$$\alpha(\omega) = \sqrt{2}\omega\left[\sqrt{\varepsilon_1^2(\omega)+\varepsilon_2^2(\omega)} - \varepsilon_1(\omega)\right]^{1/2} \quad (2)$$

$$R(\omega) = \left|\frac{\sqrt{\varepsilon_1(\omega)+j\varepsilon_2(\omega)}-1}{\sqrt{\varepsilon_1(\omega)+j\varepsilon_2(\omega)}+1}\right|^2 \quad (3)$$

$$n(\omega) = \left[\sqrt{\varepsilon_1^2(\omega)+\varepsilon_2^2(\omega)} + \varepsilon_1(\omega)\right]^{1/2} / \sqrt{2} \quad (4)$$

$$L(\omega) = \frac{\varepsilon_2(\omega)}{\varepsilon_1^2(\omega)+\varepsilon_2^2(\omega)} \quad (5)$$

The calculated optical properties at the equilibrium lattice constant are presented in Fig. 4, for the energy range up to 77 eV. The calculated optical reflectivity is shown in Fig. 4 (a). From the Fig. 4 (a), we can find that the reflectivity starts at about 70 % and has a maximum value of roughly 99 % at about 11 eV. Other peaks are situated at about 3.78 eV and 44 eV, respectively.

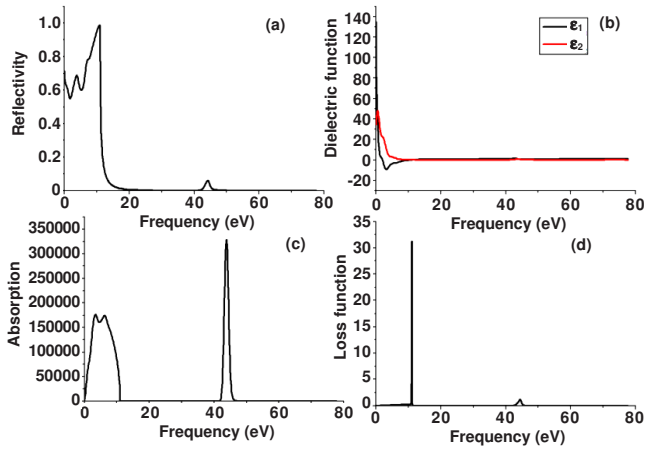

Fig. 4. Reflectivity (a), dielectric function (b), absorption coefficient (c) and electron energy-loss function (d) for Ni_2CrAl intermetallic compound

Fig. 4 (b) shows the real and imaginary parts of the dielectric function for Ni_2CrAl. The calculated imaginary part ε_2 exhibits a peak located at 0.52 eV. For the real part ε_1 spectrum the minimum is at about 3.16 eV.

From the Fig. 4 (c), we find the absorption coefficient is increased with the increase of energy from 0 eV to 3.4 eV, 4.6 eV to 6.2 eV and 41.0 eV to 43.8 eV, respectively. There are two peaks situated in the range of 0 eV to 10 eV. A very sharp peak lies in 43.8 eV.

In Fig. 4 (d), it is shown that the electron energy-loss function (ELF). Energy-loss function is an important factor describing the energy loss of a fast electron traversing in the material[26]. The peaks in ELF spectrum represent the characteristic associated with the plasma resonance and the corresponding frequency is the so-called plasma frequency ω_P[27]. The peaks of ELF correspond to the trailing edges in the reflection spectrum, for instance, the peak of ELF is at about 11 eV corresponding the abrupt reduction of reflectivity.

TABLE-1
CALCULATED ELASTIC CONSTANTS C_{ii} (GPa) AND BULK MODULUS B (GPa), SHEAR MODULUS G (GPa), YOUNG'S MODULUS Y (GPa), POISSON'S RATIO μ, (GPa) AND ANISOTROPY FACTOR A FOR Ni_2CrAl INTERMETALLIC COMPOUND

Phase	B	G	B/G	Y	μ	A	C_{11}	C_{12}	C_{44}
Ni_2CrAl	187.4	40.7	4.60	113.9	0.49	2.2	192.7	184.8	117.4

Elastic properties and mechanical stability: The elastic constants of solids provide a link between the mechanical and dynamics and provide important information concerning the nature of the forces operating in solids. In particular, they provide information on the stability and stiffness of materials. In present study, the elastic properties of Ni_2CrAl have already been obtained by the DFT calculations. The calculated elastic constants and bulk modulus are shown in Table-1. Our calculated value of the bulk modulus B from the elastic constants [$B=(C_{11}+2C_{12})/3$] is 187.4 GPa; this is the same value as that obtained from fitting the equation of state. This might be an estimate of the reliability and accuracy of our calculated elastic constants for Ni_2CrAl. Then we study the mechanical stability of Ni_2CrAl by elastic constants. The mechanical stability leads to restriction equations on the elastic constants, which for cubic crystal[28] are as follows:

$$\begin{aligned} C_{11} &> 0 \\ C_{44} &> 0 \\ C_{11} - C_{12} &> 0 \\ C_{11} + 2C_{12} &> 0 \end{aligned} \quad (6)$$

It can be seen from Table-1 that the elastic constants of the Ni_2CrAl cubic structure satisfy all the above restriction equations. This demonstrates that Ni_2CrAl is mechanically stable.

Young's modulus (Y) and Poisson's ratio (μ) are major elasticity related characteristic property for a material and are calculated using the following relations[29]:

$$Y = \frac{9GB}{3B+G} \quad (7)$$

$$\mu = \frac{1}{2}\left[\frac{B-(2/3)G}{B+(1/3)G}\right] \quad (8)$$

where, G is the isotropic shear modulus in the from $G = (G_V + G_R)/2$. G_V and G_R are Voigt's and Reuss's shear moduli, respectively and expressed as[30]:

$$G_V = \frac{C_{11} - C_{12} + 3C_{44}}{5} \quad (9)$$

$$G_R = \frac{5(C_{11} - C_{12})C_{44}}{4C_{44} + 3(C_{11} - C_{12})} \quad (10)$$

Young's modulus is often used to provide a measure of stiffness of a solid, *i.e.*, the larger is the value of Y, the stiffer is the material. Poisson's ratio provides more information about the characteristic of the bonding forces than any of the other elastic constant 0.25 and 0.5 are the lower and upper limits for central force solids, respectively[31]. The calculated Young's modulus and Poisson's ratio of the compound, based on the above expression, are listed in Table-1. From Table-1, we find the obtained value of μ is 0.49 smaller than the high limit 0.5 and larger than the low limit 0.25, indicating that the interatomic force of Ni_2CrAl is central force.

Shear modulus G represents the resistance to plastic deformation, while B represents the resistance to fracture[32]. To investigate the brittleness and ductility properties of Ni_2CrAl, the ratio of bulk modulus to shear modulus, B/G, has also been calculated. The value of B/G can classify materials as ductile or brittle by Pugh's empirical relationship[33]. If B/G > 1.75, the material behaves in a ductile manner; otherwise the material behaves in a brittle manner. From the computations, the value of B/G is 4.6 larger than 1.75. So Ni_2CrAl is considered as ductile material at ambient conditions.

The elastic anisotropy of crystal has an important implication in engineering science since it is highly correlated with the possibility to induce microcracks in materials[34]. The anisotropy factor $A = (2C_{44} + C_{12})/C_{11}$ has been evaluated to provide insight on the elastic anisotropy factor. The value of A equals 1 for an isotropic crystal, while any value smaller or larger than 1 indicates anisotropy. The magnitude of a deviation from 1 is a measure of the degree of elastic anisotropy possessed by the crystal. As can be seen from Table-1, Ni_2CrAl can not considered as elastically isotropic crystal because the value of A is larger than 1.0.

Conclusion

In summary, the physical properties of Ni_2CrAl intermetallic compound with non-Heusler phase have been studied by using first-principles calculations. The calculated lattice constants are in good agreement with available experimental data. Other main results and conclusions can be summarized as follows:

(a) The calculated electronic and band properties predict that Ni_2CrAl is a conductor.

(b) The reflectivity starts at about 70 % and has a maximum value of roughly 99 % at about 11 eV, which indicate Ni_2CrAl can strongly reflect the radiation.

(c) The calculations for elastic constants show that Ni_2CrAl can be considered as elastically isotropic and mechanically stable. The calculated value of B/G is 4.6 larger than 1.75 revealing that it may be applied as a ductile material.

ACKNOWLEDGEMENTS

The work is supported by 863 project of China (Grant No. 2009AA035002).

REFERENCES

1. J.M.D. Coey and H. Sun, *J. Magn. Magn. Mater.*, **87**, 251 (1990).
2. Y.N. Koval, G.S. Firstov and A.V. Kotko, *Scripta. Metall. Mater.*, **27**, 1611 (1992).
3. Y. Yu, J. Zhou, J. Chen, H. Zhou, C. Guo and B. Guo, *Intermetallics*, **18**, 871 (2010).
4. D.M. Gualtieri, K. Narasimhan and T. Takeshita, *J. Appl. Phys.*, **47**, 3432 (2009).

5. A.T. Yokobori Jr., M. Yoshida, M. Shibata, R. Sugiura and A. Fuji, *Strength, Fract. Complex.*, **5**, 117 (2009).
6. I.E. Gunduz, K. Fadenberger, M. Kokonou, C. Rebholz and C.C. Doumanidis, *Appl. Phys. Lett.*, **93**, 134101 (2008).
7. J.H. Yang and C.M. Wayman, *Mater. Lett.*, **16**, 254 (1993).
8. H. Choe and D.C. Dunand, *Acta. Mater.*, **52**, 1283 (2004).
9. C. Jiang, D.J. Sordelet and B. Gleeson, *Scripta. Mater*, **54**, 405 (2006).
10. A. Kumar, M. Nasrallah and D.L. Douglass, *Oxid. Met*., **8**, 227 (1974).
11. V.A. Dinh, K. Sato and H. Katayama-Yoshida, *J. Supercond. Nov. Magn.*, **23**, 75 (2010).
12. X.Q. Chen, X. Lu, D.Y. Wang and Z.X. Qin, *Smart Mater. Struct.*, **17**, 065030 (2008).
13. Y. Chieda, T. Kanomata, K. Fukushima, K. Matsubayashi, Y. Uwatoko, R. Kainuma, K. Oikawa, K. Ishida, K. Obara and T. Shishido, *J. Alloys Compd.*, **51** (2009).
14. A. Kellou, N.E. Fenineche, T. Grosdidier, H. Aourag and C. Coddet, *J. Appl. Phys.*, **94**, 3292 (2003).
15. H. Faraoun, H. Aourag, C. Esling, J.L. Seichepine and C. Coddet, *Comput. Mater. Sci.*, **33**, 184 (2005).
16. H. Rached, D. Rached, R. Khenata, A.H. Reshak and M. Rabah, *Phys. Status Solidi B*, **246**, 1580 (2009).
17. F. Yang, J.W. Wang, J.L. Ke, Z.G. Pan and B.Y. Tang, *Phys. Status Solidi B,* **248**, 2097 (2011).
18. M.D. Segall, P.J.D. Lindan, M.J. Probert, C.J. Pickard, P.J. Hasnip, S.J. Clark and M.C. Payne, *J. Phys.: Cond. Mater.*, **14**, 2717 (2002).
19. P. Hohenberg and W. Kohn, *Phys. Rev.*, **136**, B864 (1964).
20. W. Kohn and L.J. Sham, *Phys. Rev. A*, **140**, 1133 (1965).
21. D. Vanderbilt, *Phys. Rev. B*, **41**, 7892 (1990).
22. H.J. Monkhorst and J.D. Pack, *Phys. Rev. B*, **13**, 5188 (1976).
23. J.P. Perdew, S. Burke and M. Ernzerhof, *Phys. Rev. Lett.*, **80**, 891 (1998).
24. K.H.J. Buschow, P.G. Van Engen and R. Jongebreur, *J. Magnetism, Magnetic Mater*., **38**, 1 (1983).
25. S. Saha and T.P. Sinha, *Phys. Rev. B*, **62**, 8828 (2000).
26. P.D. Borges, L.M.R. Scolfaro, H.W. Leite Alves and E.F. da Silva, *Theor. Chim. Acta*, **126**, 39 (2010).
27. M. Fox, Optical Properties of Solids, Academic Press, New York (1972).
28. J.F. Nye, Physical Properties of Crystals: Their Representation by Tensors and Matrices, Oxford University Press, USA (1985).
29. B. Mayer, H. Anton, E. Bott, M. Methfessel, J. Sticht and P.C. Schmidt, *Intermetallics*, **11**, 23 (2003).
30. Y.O. Ciftci, K. Çolakoglu, E. Deligoz and H. Ozisik, *Mater. Chem. Phys.*, **108**, 120 (2008).
31. H.Z. Fu, D.H. Li, F. Peng, T. Gao and X.L. Cheng, *Comput. Mater. Sci.*, **44**, 774 (2008).
32. G. Vaitheeswaran, V. Kanchana, R.S. Kumar, A.L. Cornelius, M.F. Nicol, A. Savane, A. Delin and B. Johansson, *Phys. Rev. B*, **76**, 014107 (2007).
33. S.F. Pugh, *Philos. Magaz. Series*, **45**, 823 (1954).
34. V. Tvergaard and J.W. Hutchinson, *J. Am. Ceram. Soc.*, **71**, 157 (1988).